Nanotechnology **11** (2000) 165–168. Printed in the UK PII: S0957-4484(00)11809-4

Nanomechanical vibrating wire resonator for phonon spectroscopy in liquid helium

Andreas Kraus, Artur Erbe and Robert H Blick

Centre for NanoScience and Sektion Physik, Ludwig-Maximilians-Universität, Geschwister-Scholl-Platz 1, 80539 Munich, Germany

Received 11 February 2000, in final form 1 June 2000

Abstract. We demonstrate how to machine a vibrating wire resonator for ultrasonic excitations in gaseous and liquid helium. This novel resonator is designed as a nanoscopic mechanically flexible bridge machined out of a semiconductor/metal hybrid. Quenching of the mechanical resonance around 100 MHz in gaseous and liquid ^{4}He at 4.2 K is shown.

Vibrating wire resonators (VWRs) are standard bolometers for the quantum fluids ^{3}He/^{4}He [1]. The operating principle is to immerse a metallic wire in superfluid helium and induce a mechanical vibration by applying a magnetic field while simultaneously sending an alternating current through the wire. Usually these wires resonate at several kilohertz with deflections of the order of some micrometres. Applying superconducting cavities it is possible to probe superfluid ^{4}He [2].

Here we present a new approach for building such phonon radiators, which can be applied for spectroscopy of these quantum liquids. In contrast to previous resonators operating in the kilohertz range [3], we focus on the realization of wires or more specifically on suspended hybrid Si/metal beams with nanometre-sized dimensions and hence resonance frequencies up to 1 GHz [4, 5]. This is of great interest, since the acoustical wavelength at 100 MHz is of the order of the size of the resonator. Hence, the nanomechanical resonator can function as an ultrasonic radiator. We will first discuss the processing of the nanostructures and then proceed to the experimental setup. Moreover, we show measurements which allow us to calibrate the attenuation of the nano-VWR in liquid ^{4}He.

The beams are machined from commercially available silicon-on-insulator (SOI) wafers with a top layer thickness of 205 nm and a sacrificial layer of 400 nm. Optical lithography and evaporation of 180 nm NiCr-Au/Ti are used to define the necessary bond pads and an etch mask (Ti), which is then removed in the wet etch step. An electron beam writer (JEOL 6400) is used to define the nanomechanical resonator, consisting finally of the metallic line on top (Au) of the Si supporting membrane. In the following step the sample is etched in a reactive ion etcher (RIE) using CF_4 as an etchant. The section of the sample which is not covered by metal is milled down by 200 nm. Finally the sacrificial layer is removed using diluted (2%) hydrofluoric acid (HF) at an etch rate of 10 nm s^{-1}.

In the right inset of figure 1 the suspended beam is shown in a scanning electron beam micrograph: the bridge is freely suspended between two tuning gates, which can be coupled capacitively. The beam has a length of 1 μm and a width of 200 nm, and the gates are covered by a 50 nm Au layer. The gates can be applied to tune the mechanical resonance by biasing up to about 10 V. For the measurements we employ a Hewlett–Packard network analyser (HP 8751A), which allows us to monitor amplitude and phase of the resonator simultaneously with 1 Hz resolution. The beam's resonance is excited by the alternating current at radiofrequencies and the static magnetic field applied in plane. At resonance a magnetomotive force is induced, which in turn can be read out. In our case, the reflection of the signal is determined. For sensitive detection of the reflected signal, a high-gain (15 dB) amplifier is brought into the line feeding the circuit†. The amplifier is optimized for a frequency response between 1 and 500 MHz. The impedance of the coaxial cables and the leads in the sample holder is 50 Ω; the dc resistance of the sample is found to be 30 Ω, thus a fairly good impedance matching is guaranteed. The vibrating wire in turn induces an electromagnetic field, which is amplified and measured with the network analyser [5].

First we measured resonance curves characterizing the elastic properties of the beam in linear (marked L in figure 1) and nonlinear (marked NL) response. While the resonator shows a Lorentzian line shape in the linear regime, the nonlinear regime is characterized by an S-shaped curve with a strong hysteresis. The resonance frequency is around 96 MHz at 4.2 K and shifts to lower values when the resonator enters the nonlinear regime. The reflection coefficient is defined by

$$r = \frac{P_{\mathrm{out}}}{P_{\mathrm{in}}};$$

† In these measurements the network analyser compared a reference channel with an ideal load with the signal reflected from the nanoresonator. In order to achieve optimum operation the reference channel and signal channel are connected to high-gain amplifiers (double-sided amplifier).

0957-4484/00/030165+04$30.00

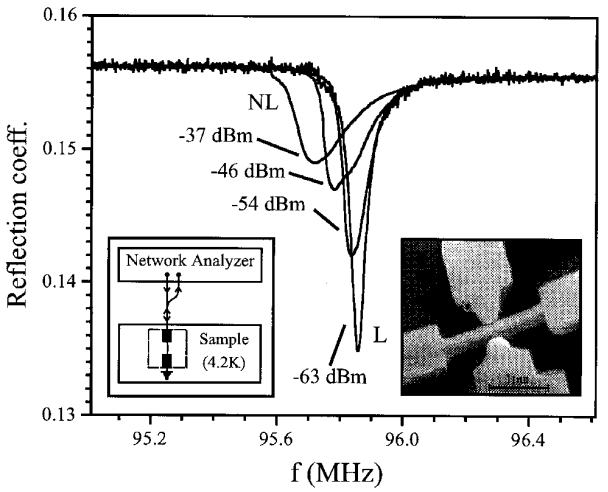

Figure 1. The fundamental resonance of the Si/Au beam as seen in the reflection coefficient of the beam from the linear (L) into the nonlinear (NL) regime at 4.2 K and 20 mbar He gas pressure. Left inset: circuit diagram of the experimental setup. The reflected signal is amplified and detected by the network analyser. Inset on the lower right: scanning electron beam micrograph of the VWR. The suspended beam consists of a silicon supporting structure and a metallized top layer. The gates located on the side of the beam can be applied to electrostatically tune the beam's mechanical resonance.

obviously it decreases with increasing power. The resonator can be modelled as a typical Duffing oscillator using

$$y''(t) + \gamma y'(t) + \omega_0^2 y(t) + k_3 y^3(t) = A\sin(\omega t), \qquad (1)$$

where y is the displacement, $f_0 = \omega_0/2\pi$ the eigenfrequency of the beam, $\gamma = \omega_0/Q = 4.5 \times 10^5\ \mathrm{s}^{-1}$ represents the damping constant and the driving amplitude is given by $A = 1.4 \times 10^5\ \mathrm{m\,s}^{-2}$ at -63 dB m and $2.8 \times 10^6\ \mathrm{m\,s}^{-2}$ at -37 dB m. The shift to lower frequencies implies that $k_3 < 0$ in the Duffing equation. Attenuation commonly shifts the eigenfrequency of a linear resonator to lower frequencies and deteriorates the quality factor. In the measured resonator a quality factor of $Q \sim 2 \times 10^3$ was determined.

Figure 2(a) shows the measurement of the reflected power during filling of the sample holder with ^{4}He when the wire is driven in the linear response regime. The sample holder was cooled to 4.2 K. The attenuation by the gas leads to a decrease of the resonance amplitude, a shift to lower frequencies and a broadening of the resonance. When liquefaction of ^{4}He occurs (shown in the last trace), the resonance disappears completely. As seen in this figure we find even in the linear regime of the resonator's response a dispersion when the ^{4}He content is increased. This corresponds to an effective momentum transfer to the ^{4}He atoms impinging onto the resonator. To estimate this momentum transfer we calculate the number of accelerated ^{4}He atoms via $pV = NkT$. The volume V is determined by the oscillation amplitude of the beam. The momentum transfer per atom is found to be 3×10^{-20} N s at $p \cong 690$ mbar, $T = 4.2$ K (at an excitation power of the network analyser of -68 dB m).

Increasing the power applied to the resonator a non-zero amplitude of the resonator is found (see figure 2(b)).

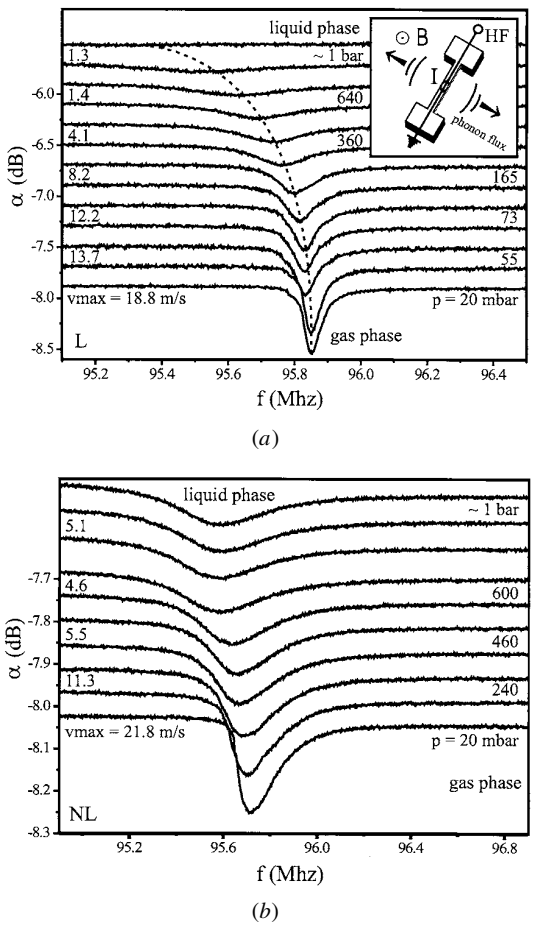

Figure 2. (a) Attenuation of the mechanical resonance amplitude by increasing ^{4}He pressure as indicated until liquefaction occurs in the linear (L) regime (-63 dB m input power, $T = 4.2$ K). The maximum velocity of the beam $v_{\max}$ has been calculated for each curve and is given on the left-hand side. In the inset a schematical view for directed phonon generation is sketched. The magnetic field is oriented perpendicular to the high-frequency current I. (b) Resonance traces of the beam in the nonlinear (NL) regime at different ^{4}He fillings (4.2 K). Again the maximum velocity of the beam has been calculated. The motion is not suppressed completely in liquid ^{4}He, thus allowing vibrational excitations.

Repeating the measurement in the nonlinear regime enables us to observe the motion of the beam even in the liquid phase. This measurement is depicted in figure 2(b): the bottom six curves are taken in ^{4}He gas while the top four curves are taken in the liquid phase. The traces change dramatically in the gaseous phase above 10 mbar, since with increasing pressure the attenuation of the beam's motion is increased due to the scattering of ^{4}He atoms. On the other hand damping in the liquid depends on the viscosity, which does not change when supplying more helium. Thus the curves change only slightly when the beam is immersed in the liquid phase. Hence, we show that it is possible to create excitations in liquid ^{4}He, when operating the wire in the nonlinear regime. It should be noted that this damping might also be explained by the transverse acoustic impedance $\mathcal{Z} = \rho v_L$, where ρ is the helium density and v_L the velocity of sound as shown by Lea *et al* [6]. To address this question a variety of different beam geometries have to be built. However, in principle the plane

of phonon emission can be chosen according to the direction of the magnetic field, as sketched in the inset of figure 2(*a*). In the present case the magnetic field was applied perpendicular to the plane of the sample, hence excitations are propagating in-plane away from the beam. Obviously the electrodes in the current setup disturb the free propagation of phonons. This might cause a back-flow and hence turbulences in the heat flow.

It is especially interesting to use the nano-resonators for creating excitations in superfluid helium, since the motion of the beam is of the same order as the critical velocity in ^{4}He. Until the beam reaches this velocity vortex line generation is considered to be low [7]. It has to be noted that losses into sound waves are still possible below the critical velocity. Further acceleration leads to the excitation of vortex states in the fluid resulting in an increased energy consumption. This can be seen in a flattening of the resonance curves. In ^{3}He the critical velocity is given by the energy required for pair breaking the superfluid pairs, which is in the mm s^{-1} range [1]. In ^{4}He it is given by the creation of vortex states at low pressures and the excitation of rotons at higher pressures. The corresponding velocities for these excitations are about 25 m s^{-1}. In cold-neutron scattering experiments [8] even the zero-pressure critical velocity has been measured ($v_c = 60$ m s^{-1}). Therefore vibrating wire experiments have only been successful in ^{3}He, while in ^{4}He the critical velocity has been reached with accelerated charged ions only [9].

In order to verify that we are able to reach the critical velocities, we monitored the velocities of the beam depending on the input power and the amount of ^{4}He in the sample holder. We did this by calculating the maximum amplitude $Y_{0,\max}$ during one cycle of the oscillation using the equation

$$Y_{0,\max} = \frac{lBI_0}{2m_{\text{eff}}\omega_0\mu}. \tag{2}$$

Here $Y_{0,\max}$ gives the maximum displacement of the beam perpendicular to the magnetic field and $\mu = 2.23 \times 10^5$ s^{-1} is the damping coefficient of the mechanical system. $l = 2L/\pi = 1.165$ μm and $m_{\text{eff}} = 3.418 \times 10^{-16}$ kg are the effective length and effective mass of the resonator respectively, and B is the magnetic field. The amplitude of the input current at -63 dB m is $I_0 = 4.09 \times 10^{-6}$ A and at -37 dB m it is 8.16×10^{-5} A. Subsequently we obtain $Y_{0,\max} = 9.79$ nm. The parameters of the Duffing equation (1) can be extracted from the measurements in the nonlinear regime. The velocity is then estimated via

$$v \propto fY_{0,\max}.$$

In the linear regime we find a linear dependence on the input power as long as no ^{4}He gas is added. The maximum velocity in this case is 20 m s^{-1}. When filling with ^{4}He, this velocity is decreased until it finally reaches zero in the case of liquid helium (see figure 2). In the nonlinear regime we begin at a velocity of 20 m s^{-1}, which is then reduced to 5 m s^{-1} in the liquid. The decrease of the velocity is mainly due to the deterioration of the quality factor. To reach the critical velocities in ^{4}He we have to increase the velocity by a factor of five, which is possible by simply scaling down the resonator in size. The smallest resonators fabricated to date in silicon have widths of only 80 nm [10] and 25 nm [11] and a length of ∼700 nm.

A small drawback of this resonator so far is the non-superconducting metal on top of the nanobridge. A crude estimation of the Joule heating dissipated by the wire yields an energy of $\sim 1.1 \times 10^{-20}$ J per cycle, while the energy for excitations in superfluid ^{4}He is of the order of $\sim 3 \times 10^{-23}$ J. Hence, we observe mostly isotropic radiation and not ballistic phonon emission, as sketched in the ideal case of figure 2(*a*). This problem might be overcome by using a superconducting metal on top of the suspended beam. However, from the data we obtained so far we can conclude that it should be possible to create excitations in the liquid state. Clearly, more detailed experiments are needed to give a conclusive answer.

In summary we presented measurements on nanomechanical resonators in gaseous and liquid ^{4}He. These measurements demonstrate strong attenuation of the mechanical excitations of the resonator. Since the displacement can be tuned even in the liquid, the resonators can be applied as nano-VWR in order to create vortex state and roton excitations in superfluid ^{4}He and ^{3}He. In recent experiments quantum effects in superfluid ^{3}He analogous to the Josephson effect have been found [12]. In order to observe quantum effects, the objects moving in the liquid have to be smaller than the superfluid healing length. This length, which determines the width of the vortex states as well [13, 14], is about 50 nm in superfluid ^{3}He. As noted before silicon beams with a width of 80 nm have already been fabricated [11]. Thus quantum effects in ^{3}He are in the accessible range for these nano-VWRs. Our calculations show that the velocities required for these excitations are well in the experimentally accessible range. Although a clear signature of directed phonon or roton excitation was not yet found, we presume that, by replacing the non-superconducting metal on top of the electromechanical resonator by a superconducting one, we will obtain new insight into the excitation mechanisms of quantum fluids on a nanoscopic scale.

Furthermore, since a frequency range of 1 GHz seems to be a realistic goal with current lithography, velocities up to ten times larger than what we achieved are possible. Thus even the regime of roton excitations might be accessible. Another future experiment is to determine the dispersion relation of phonons in ^{4}He [15]. For the low-energy excitations the dispersion is purely acoustical up to frequencies of some 100 GHz. It is therefore possible to determine the dispersion of these excitations in the low-energy limit ranging from some Megahertz up to possibly 1 GHz. Moreover, the eigenfrequency of the nanoresonators can easily be varied by a tuning gate. Hence these nanoresonators can also be considered as ultrasonic generators. However, a more intricate setup is required to probe excitation of ultrasonic waves in liquid ^{4}He.

Acknowledgments

We would like to thank J P Kotthaus for his support and W Zwerger, P Leiderer and A Wixforth for discussions. Also we would like to thank W Schoepe and N Hecker for critically reading the manuscript and S Manus for technical

help. This work was funded in part by the Deutsche Forschungsgemeinschaft (DFG).

References

[1] Castelijns C A M, Coates K F, Guénault A M, Mussett S G and Pickett G R 1985 *Phys. Rev. Lett.* **56** 69
Castelijns C A M, Coates K F, Guénault A M, Mussett S G and Pickett G R 1986 *Phys. Rev. Lett.* **56** 69–72
Fisher S N, Guénault A M, Kennedy C J and Pickett G R 1991 *Phys. Rev. Lett.* **67** 3788–91
Fisher S N, Guénault A M, Kennedy C J and Pickett G R 1992 *Phys. Rev. Lett.* **69** 1073

[2] Jäger J, Schuderer B and Schoepe W 1995 *Phys. Rev. Lett.* **74** 566

[3] Triqueneaux S, Collin E, Cousins D J, Fournier T, Baeuerle C, Bunkov Y M and Godfrin H 2000 *Physica* B at press

[4] Cleland A N and Roukes M L 1996 *Appl. Phys. Lett.* **69** 2653
Carr D W and Craighead H G 1997 *J. Vac. Sci. Technol.* B **15** 2760

[5] Krömmer H, Erbe A, Tilke A, Manus S and Blick R H 2000 *Europhys. Lett.* **50** 101
(Krömmer H, Erbe A, Tilke A, Manus S and Blick R H 1999 *Preprint* cond-mat/9910334)

[6] Lea M J, Fozooni P and Retz P W 1984 *J. Low Temp. Phys.* **54** 303
Lea M J and Fozooni P 1986 *J. Low Temp. Phys.* **62** 55
Lea M J, Retz P W and Fozooni P 1987 *J. Low Temp. Phys.* **66** 325

[7] Landau L D and Lifschitz E M 1990 *Lehrbuch der Theoretischen Physik, Band IX, Statistische Physik 2, Statistik des Festkörpers* (Berlin: Akademie)

[8] Henshaw D G and Woods A D B 1960 *Proc. 7th Int. Conf. on Low-Temperature Physics (Toronto, 1960)*

[9] Rayfield G W 1966 *Phys. Rev. Lett.* **16** 934

[10] Pescini L, Tilke A, Blick R H, Kotthaus J P, Eberhardt W and Kern D 1999 *Nanotechnology* **10** 418

[11] Blick R H, Erbe A, Tilke A and Wixforth A 2000 *Phys. Blaetter* **1** 31
Tilke A, Pescini L, Erbe A, Lorenz H and Blick R H 2000 at press

[12] Pereverzev S V, Loshak A, Backhaus S, Davis J C and Packard R E 1997 *Nature* **388** 449
Backhaus S, Pereverzev S, Simmonds R W, Loshak A, Davis J C and Packard R E 1998 *Nature* **392** 687

[13] Tilley D R and Tilley J 1990 *Superfluidity and Superconductivity* (New York: Hilger)

[14] Packard R E 1998 *Rev. Mod. Phys.* **70** 641

[15] Wyatt A F G, Tucker M A H and Cregan R F 1995 *Phys. Rev. Lett.* **74** 5236